

1-1-2016

# Magnetospheric Ion Influence On Magnetic Reconnection At The Duskside Magnetopause

S. A. Fuselier

J. L. Burch

P. A. Cassak

J. Goldstein

AGU PUBLICATIONS

Geophysical Research Letters

RESEARCH LETTER
10.1002/2015GL067358

Special Section:
First Results from NASA's Magnetospheric Multiscale (MMS) Mission

# Magnetospheric ion influence on magnetic reconnection at the duskside magnetopause

S. A. Fuselier[1,2], J. L. Burch[1], P. A. Cassak[3], J. Goldstein[1,2], R. G. Gomez[1], K. Goodrich[4], W. S. Lewis[1], D. Malaspina[4], J. Mukherjee[1], R. Nakamura[5], S. M. Petrinec[6], C. T. Russell[7], R. J. Strangeway[7], R. B. Torbert[1,8], K. J. Trattner[4], and P. Valek[1,2]

[1]Southwest Research Institute, San Antonio, Texas, USA, [2]University of Texas at San Antonio, San Antonio, Texas, USA, [3]Department of Physics and Astronomy, West Virginia University, Morgantown, West Virginia, USA, [4]Laboratory for Atmospheric and Space Physics, University of Colorado Boulder, Boulder, Colorado, USA, [5]Space Research Institute, Austrian Academy of Sciences, Graz, Austria, [6]Lockheed Martin Advanced Technology Center, Palo Alto, California, USA, [7]Institute of Geophysics and Planetary Physics, University of California, Los Angeles, California, USA, [8]Space Science Center and Department of Physics, University of New Hampshire, Durham, New Hampshire, USA

**Key Points:**
- Magnetospheric ions have significant density at the magnetopause
- Magnetospheric ions do not influence reconnection significantly at the duskside magnetopause

**Correspondence to:**
S. A. Fuselier,
sfuselier@swri.edu

**Citation:**
Fuselier, S. A., et al. (2016), Magnetospheric ion influence on magnetic reconnection at the duskside magnetopause, *Geophys. Res. Lett.*, *43*, 1435–1442, doi:10.1002/2015GL067358.

Received 9 DEC 2015
Accepted 8 FEB 2016
Accepted article online 11 FEB 2016
Published online 29 FEB 2016

**Abstract** Magnetospheric ions from the ring current, warm plasma cloak, and the plasmaspheric drainage plume all interact with the dusk flank magnetopause. During periods of strong magnetospheric convection, these ions may contribute significantly to the magnetospheric mass density at the magnetopause. Observations from the Magnetospheric Multiscale mission Hot Plasma Composition Analyzer at the duskside magnetopause near reconnection X lines show that ions from the ring current and warm plasma cloak may have high mass densities. However, these mass densities are not as large as the mass density in the magnetosheath. The results suggest that except for possible influence from the plasmaspheric drainage plume, the other major magnetospheric ion populations do not greatly influence asymmetric reconnection at the duskside magnetopause.

## 1. Introduction

Magnetic reconnection is ubiquitous at the Earth's magnetopause for all interplanetary magnetic field (IMF) orientations (see, e.g., recent reviews by *Fuselier and Lewis* [2011] and *Cassak and Fuselier* [2015]). Reconnection across the magnetopause is highly asymmetric because the plasma mass density in the magnetosphere is typically much lower than the mass density in the magnetosheath [e.g., *Fuselier et al.*, 1993], and the magnetic field strength is higher in the magnetosphere. This asymmetry has important implications on the structure and rate of reconnection at the magnetopause [*Cassak and Shay*, 2007].

Although the magnetospheric mass density is typically low, there are times and locations at the magnetopause when this density may rival the magnetosheath mass density. At least three broadly defined ion populations may contribute significantly to the magnetospheric mass density; the magnetospheric ring current, the "warm plasma cloak", and the plasmaspheric drainage plume. These populations are observed at times at the dusk flank magnetopause (see Figure 1) and are usually distinguishable by their energies and composition.

The ring current is a medium-energy (~3–100 keV) population consisting of $H^+$, $He^{2+}$, $O^+$, and $He^+$. Ion concentrations vary with magnetospheric activity. During relatively quiet times, $H^+$ dominates with lower concentrations of the other ions. During active times, when magnetospheric convection is enhanced, $O^+$ can dominate. The lower energy ring current ions (~3–30 keV) gradient drift to the duskside magnetopause as depicted schematically in Figure 1.

The warm plasma cloak [e.g., *Chappell et al.*, 2008] is a lower energy (~10 eV to 3 keV) ionospheric outflow population that propagates from high latitudes into the magnetotail. The composition reflects that of ionospheric outflow: $H^+$, $O^+$ and, to a lesser extent, $He^+$ [*Yau et al.*, 1984; *Collin et al.*, 1988]. Similar to the ring current, $H^+$ is often dominant, but $O^+$ can dominate ionospheric outflow during active times. The warm plasma cloak convects sunward either directly to the dawnside magnetopause or around the dawnside to the duskside magnetopause [e.g., *Chappell et al.*, 2008] as depicted in Figure 1. The occurrence frequency is higher on the dawnside versus the duskside, although the density dependence at the magnetopause with local time is not known.

The plasmaspheric drainage plume is a low energy (typically $<1$ eV) ionospheric population that is an extension of the plasmasphere on the duskside magnetosphere, as depicted in Figure 1. Its composition reflects that of

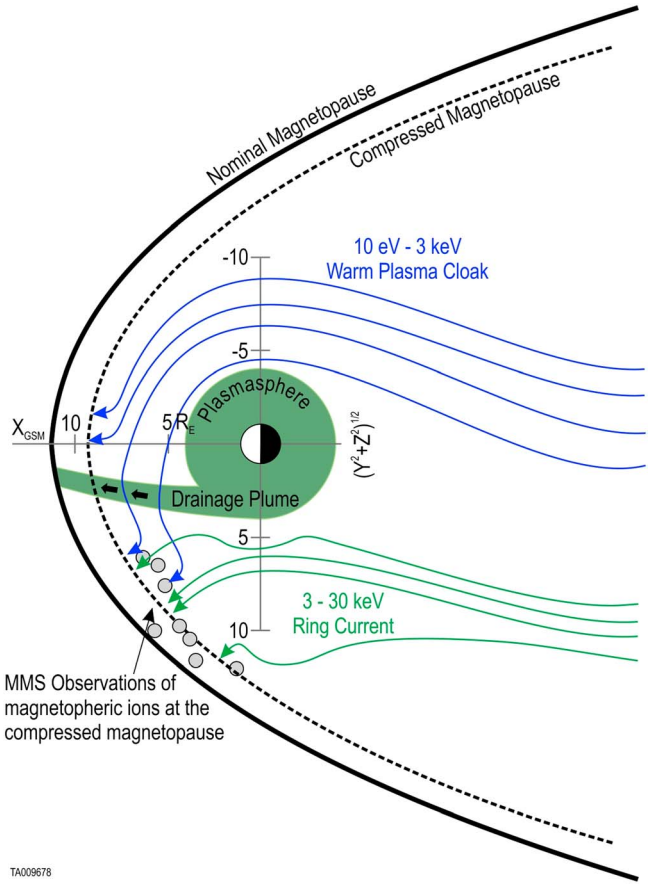


**Figure 1.** Schematic representation of magnetospheric plasma at the duskside magnetopause. Three populations, the ring current, warm plasma cloak, and plasmspheric drainage plume, all convect to the duskside magnetopause. The grey dots show the location of eight MMS magnetopause crossing events. Ion composition measurements from these events are used to determine the effect of magnetospheric ions on magnetopause reconnection.

the plasmasphere: $H^+$, $He^+$, and, to a lesser extent, $O^+$. The plume and the duskside outer plasmasphere may have higher temperature (tens of eV) [e.g., *Olsen et al.*, 1987; *Labelle et al.*, 1988].

These magnetospheric ion populations may have high mass densities. For example, plasmaspheric material has been observed adjacent to the magnetopause with densities $>10\,cm^{-3}$ [*Su et al.*, 2000; *McFadden et al.*, 2008; *Walsh et al.*, 2014a, 2014b]. $H^+$, $He^+$, and $O^+$ were identified in the magnetopause boundary layers because these ion populations were cold and streaming with the $\mathbf{E}\times\mathbf{B}$ velocity in the layer [e.g., *Gosling et al.*, 1990]. The high density and heavy ion content of these populations led to the suggestion that magnetospheric ions may modify (reduce) the reconnection rate at the magnetopause [e.g., *Borovsky and Denton*, 2006; *Borovsky et al.*, 2013].

Connecting magnetospheric ion populations with modification of reconnection at the magnetopause is not straightforward. There are at least two complications to this connection. The first complication is that mass spectrometry measurements are required to determine the mass densities from the three magnetospheric ion populations. Ion species in the plasmaspheric plume are sometimes identifiable in the boundary layers using instrumentation that has energy analysis only. However, the plasmaspheric plume does not always remain cold [e.g., *Labelle et al.*, 1988], necessitating mass spectrometry measurements. Furthermore, the other two populations have higher temperature and require instrumentation that resolves mass. Only a few space missions have had mass spectrometers capable of measuring all magnetospheric ion populations near the magnetopause and measurements from these missions are limited [see, e.g., *Fuselier et al.*, 1993; *Fuselier*, 1995; *Wang et al.*, 2015].

The second complication is that in situ measurements must be obtained near the magnetopause reconnection X line. There is ample evidence that magnetospheric ions flow through the open magnetopause into the magnetosheath [e.g., *Sonnerrup et al.*, 1981; *Fuselier et al.*, 1991; *Su et al.*, 2000]. However, simply crossing the open magnetopause does not necessarily indicate that these magnetospheric ions were near the reconnection X line and therefore may have influenced the reconnection process.

The purpose of this paper is to present new, mass-resolved, observations of magnetospheric and magnetosheath mass density at the dusk flank magnetopause from the Hot Plasma Composition Analyzer (HPCA) on the Magnetospheric Multiscale (MMS) Mission [*Young et al.*, 2014; *Burch et al.*, 2015]. One event near the reconnection X line is discussed in detail in the next section. This discussion is followed by analysis of several other events, also near reconnection X lines. These results show that the magnetospheric mass density at the dusk flank magnetopause rarely rivals that of the magnetosheath mass density and that even in extreme instances, the effect of two of the magnetospheric ion populations on the reconnection rate is relatively small.

## 2. Observations on 11 September 2015

During phase 1a of the MMS mission, the spacecraft orbit precesses in local time across the dayside magnetopause from the dusk to the dawn terminator [*Fuselier et al*., 2014]. The spacecraft apogee is 12 Earth radii ($R_E$), and the nominal position of the magnetopause at the terminator is ~15 $R_E$. Thus, the four MMS spacecraft cross the dusk flank magnetopause typically when the magnetosphere is compressed. Compression occurs because the solar wind dynamic pressure is high and/or the interplanetary magnetic field (IMF) has a significant southward component. Such was the case on 11 September 2015 from 0753 to 0757 UT. The solar wind density measured by the Wind spacecraft was ~12 $cm^{-3}$, and the velocity was ~480 km/s, resulting in a dynamic pressure of about 7 nPa, which is well above the nominal dynamic pressure of about 1.5 nPa. The IMF was strongly southward ($B_Z \sim -18$ nT). This combination of high dynamic pressure and strong southward IMF also resulted in strong magnetospheric convection. The 3 h *Kp* index was 7 for the time interval near 0800 UT.

Figure 2 shows HPCA and magnetometer observations from MMS3. Shown are (top to bottom) energy-time spectrograms and densities of the major ion species in the magnetosheath and magnetosphere, starting with $H^+$, followed by $He^{2+}$, $He^+$, and $O^+$. Figure 2 (bottom panel) shows the *Z* (GSM) component of the magnetic field.

There are one partial and four complete magnetopause crossings in the 4 min of data shown in Figure 2. The spacecraft starts and ends in the magnetosphere, crossing the magnetopause twice between 0754 and 0754:20 UT, making a partial crossing centered on 0755 UT and then crossing twice more between 0755:30 and 0756:10 UT. The magnetosheath and boundary layer/current layer BL/CL intervals adjacent to the magnetopause crossings are identifiable by the ~1 keV $He^{2+}$ population. In all regions, there is a persistent population of multi-keV-energy $H^+$, $He^{2+}$, $He^+$, and $O^+$. For $He^{2+}$, this population starts at about 8 keV and extends to 40 keV, the maximum energy of HPCA. This is the magnetospheric ring current population. This population may leak into the magnetosheath on open field lines. The presence of this population in the magnetosheath intervals in Figure 2 (except possibly for a very short interval near 0756 UT) indicates that the spacecraft was never far from the magnetopause.

Throughout the magnetosphere intervals, there is a population of low energy (~few eV to 100 eV) $H^+$ and moderate energy $He^+$ and $O^+$. Although the fluxes vary considerably, the population is persistent, and the average energy is proportional to mass. For $O^+$, this moderate-energy population blends almost smoothly with the $O^+$ ring current population. This population is the warm plasma cloak. $He^{2+}$ is conspicuously absent at moderate energies, indicative of the population's ionospheric origin [see, e.g., *Yau et al*., 1984; *Collin et al*. 1988].

In the magnetosphere, there is no detectable very low energy (~few eV) $He^+$ and therefore no evidence of a plasmaspheric drainage plume in the HPCA energy range. However, the plasmaspheric drainage plume is difficult to detect if it remains cold. Although MMS has active spacecraft potential control [*Torkar et al*., 2014], this control maintains the spacecraft potential at a few volts positive, and the lowest energy step for HPCA is at about 1.3 eV. Cold, slowly convecting plasmaspheric ions may not overcome the few volt spacecraft potential. As a result, the two magnetospheric populations focused on here are the ring current and the warm plasma cloak. The total plasma (number) density is determined independently from MMS plasma wave measurements [*Torbert et al*., 2014]. During the magnetospheric interval from 0753 to 0754 UT in Figure 2, the number density derived from the plasma wave measurements (not shown) was ~3 $cm^{-3}$. This density agrees reasonably well (within 50%) with the total ion density measured by HPCA. This agreement and the lack of low energy $He^+$ indicate that there was probably no substantial drainage plume plasma present at the magnetopause.

Using $H^+$ fluxes alone, it is difficult to distinguish a low-latitude boundary layer (or, more simply, a boundary layer) interval from a magnetospheric interval with a substantial warm plasma cloak population. Often, the average energy of the warm plasma cloak $H^+$ is lower than that in the boundary layer. However, this energy distinction is not always possible. For example, the magnetospheric interval centered at 0756:25 UT has a substantial $H^+$ population with an average energy similar to that of the boundary layer population centered at 0754:25 UT. The boundary layer and the warm plasma cloak are distinguished in HPCA by their different composition. The warm plasma cloak has very little $He^{2+}$ between ~1 eV and 8 keV, while the ~1 keV $He^{2+}$ concentration in the boundary layer is substantial.

Because of the large variation in the magnetospheric ion densities, all of the magnetospheric intervals in Figure 2 are used to compute an average mass density, and the peak $O^+$ magnetospheric density at 0755:35 UT is used to compute an "extreme" mass density. The density variations in the magnetosheath are less. Therefore, the two

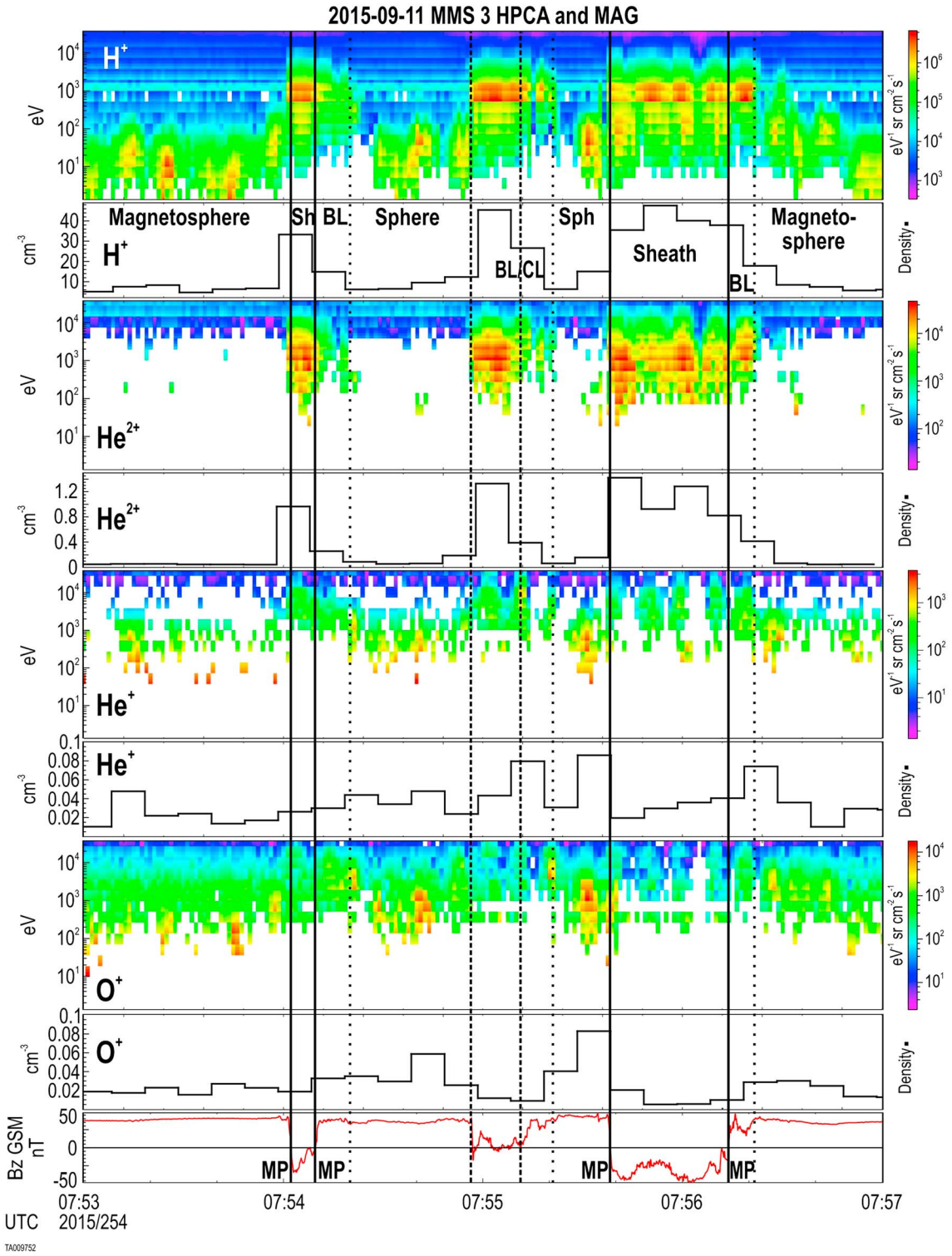


**Figure 2.** Multiple crossings of the duskside magnetopause by MMS 3 when magnetospheric ions were present. (top to bottom) Energy time spectrograms of fluxes and densities for $H^+$, $He^{2+}$, $He^+$, and $O^+$. (bottom panel) $B_z$ (GSM). High-energy (>8 keV) ring current $H^+$, $He^{2+}$, $He^+$, and $O^+$ are observed throughout the interval, and lower energy warm plasma cloak $H^+$, $He^+$, and $O^+$ are observed at variable densities in the magnetospheric intervals. The interval with the highest $O^+$ density, at 0755:35 UT, is used to determine an extreme magnetospheric ion mass density.

short magnetosheath intervals in Figure 2, between the pairs of magnetopause crossings, are used to compute an average magnetosheath mass density. The boundary layers are not used because they are a mixture of magnetospheric and magnetosheath populations, and high-energy $O^+$ in the magnetosheath is also not used in the magnetosheath mass density since it is of magnetospheric origin. Technically, this high-energy $O^+$ could contribute to the magnetosheath mass density since it is picked up by the magnetosheath flow and may convect into a reconnection site. However, the effect of this population on the magnetosheath mass density is small.

In the magnetosheath, $H^+$ dominates, but $He^{2+}$ (with a ~4% average concentration) contributes ~16% to the total, average mass density of 46 amu $cm^{-3}$. In the magnetosphere, the warm plasma cloak dominates the total mass density. For $H^+$, the ring current density is ~0.1–0.5 $cm^{-3}$, while the average $H^+$ density for the warm plasma cloak is ~7 $cm^{-3}$. The total $O^+$ density in the magnetosphere varies by almost a factor of 10 from the peak at 0755:35 UT to the lowest densities at 0753 UT in Figure 2. $H^+$ and $O^+$ contribute approximately equally to the average mass density, but in the extreme interval at 0755:35 UT, $O^+$ contributes approximately 40% more mass density than $H^+$ does. The magnetosheath mass densities and in the average and extreme magnetospheric mass densities for this event are listed in Table 1.

Figure 3 shows the location of the MMS spacecraft for the time interval in Figure 2. Plotted are shear angles between the model magnetosheath and magnetospheric fields projected onto the *Y-Z* GSM plane. High shear regions are shown in red, the highest shear regions (where the shear is >175°) are shown in white, and very low shear regions are in purple. The black circle is the terminator projected onto this plane. For this interval, the IMF was almost purely southward. The maximum shear reconnection line model [*Trattner et al*., 2007] predicts a duskside reconnection line that is located in the broad region of nearly antiparallel shear angles that extends from the southern cusp region on the noon meridian, through the dayside, and along the equator past the dusk terminator. The MMS spacecraft made multiple magnetopause crossings just south and within a few Earth radii ($R_E$) of this duskside reconnection line. Thus, magnetospheric ion populations observed in Figure 2 at the magnetopause likely interacted with the reconnection X line locally near the spacecraft and possibly at other locations along the reconnection line that runs from the noon meridian past the dusk terminator.

## 3. Other Events at the Dusk Flank Magnetopause

Seven other dusk flank magnetopause events are identified in Figure 1. These seven events have characteristics similar to the event showcased in Figure 2. All but one occurred when the spacecraft crossed the compressed magnetopause under high solar wind dynamic pressure. The events occurred for a wide range of magnetospheric convection conditions, from relatively low ($Kp = 2$) to high convection ($Kp = 7$) for the 11 September 2015 event.

All magnetopause crossings occurred relatively close to a reconnection X line. The location of this line was determined either by using the maximum shear model [*Trattner et al*., 2007] or, in two events, by identifying flow jet reversals in the boundary layer. These reversals are indicative of a reconnection line passing the spacecraft placing the spacecraft at the reconnection X line. For the other events, the accuracy of the maximum shear model is of the order of 1–2 $R_E$, so the spacecraft was always within a few $R_E$ of the X line for all events. The predicted shear at the magnetopause at the X line was large for all events (for example, see Figure 3 for the 11 September 2015 event) indicating that antiparallel reconnection was occurring near the spacecraft for all but one event. For the event on 19 September 2015 at 0742 UT, component reconnection was probably occurring near the spacecraft, but the shear was still rather large (>160°).

## 4. Estimating the Effect on Reconnection

*Borovsky et al*. [2013] used the *Cassak and Shay* [2007] and *Birn et al*. [2008] formulations of the antiparallel reconnection rate to derive a correction to the rate for nonzero magnetospheric mass density (equation (1)).

$$R = (\rho_S B_M)^{\frac{1}{2}} / (\rho_M B_S + \rho_S B_M)^{\frac{1}{2}} \quad (1)$$

where $R$ ("*M*" in the nomenclature from *Borovsky et al*. [2013]) is the fractional reduction of the local dayside reconnection rate due to the nonzero magnetospheric ion populations. In equation (1), $\rho$ is the mass density and $B$ is the reconnecting component of the magnetic field and the subscripts $M$ and "$S$" refer to

**Table 1.** Mass Correction Factors and Fractional Reduction of the Local Reconnection Rate for Eight Magnetopause Events Observed by the MMS Spacecraft

| Date | MP Time (hhmm) | $M_{sheath}$ Mass Density (amu cm$^{-3}$) | $M_{sheath}$ B Total (nT) | $M_{sphere}$ avg Mass Density (amu cm$^{-3}$) | $M_{sphere}$ avg B Total (nT) | $M_{sphere}$ Extreme Mass Density (amu cm$^{-3}$) | $M_{sphere}$ B Total for Extreme Mass Density (nT) | MC Mass Correlation Factor avg | MC Mass Correlation Factor Extreme | *R* avg | *R* Extreme | Distance to X line ($R_E$) | Model or Flow Jet Reversal | *Kp* |
|---|---|---|---|---|---|---|---|---|---|---|---|---|---|---|
| 2 Sep 2015 | 1734 | 48.7 | 18.3 | 2.6 | 24.1 | 3.1 | 24 | 0.04 | 0.04 | 0.98 | 0.98 | ~2 | Model | 2 |
| 7 Sep 2015 | 1313 | 32.5 | 35.8 | 1.2 | 32.8 | 2.5 | 35 | 0.04 | 0.09 | 0.98 | 0.96 | ~2 | Model | 5 |
| 9 Sep 2015 | 0850 | 76.7 | 33.2 | 10.1 | 38.1 | 12.5 | 38.1 | 0.10 | 0.15 | 0.95 | 0.93 | ~3 | Model | 6 |
| 10 Sep 2015 | 1232 | 59.9 | 25.9 | 2.2 | 38.9 | 2.6 | 40.7 | 0.02 | 0.03 | 0.99 | 0.99 | ~0 | Flow reversal | 2 |
| 11 Sep 2015 | 0810 | 46.1 | 72.7 | 14.8 | 95.8 | 24.7 | 93.2 | 0.29 | 0.47 | 0.88 | 0.82 | ~1 | Model | 7 |
| 14 Sep 2015 | 1546 | 20.4 | 24.6 | 1.9 | 21 | 2.5 | 21 | 0.1 | 0.15 | 0.95 | 0.93 | ~2 | Model | 5 |
| 19 Sep 2015 | 0742 | 64.1 | 55.5 | 3.0 | 54.4 | 6.7 | 58.2 | 0.05 | 0.1 | 0.98 | 0.95 | ~0 | Flow reversal | 5 |
| 19 Sep 2015 | 1210 | 45 | 43.3 | 4 | 44.1 | 4.9 | 44.7 | 0.09 | 0.1 | 0.96 | 0.95 | ~2 | Model | 2 |

the magnetosphere and magnetosheath, respectively. Continuing to follow *Borovsky et al.* [2013], *R* is rewritten as (equation (2)).

$$R = (1 + \mathrm{MC})^{-\frac{1}{2}}, \tag{2}$$

where the mass correction factor, MC, ("p" in the nomenclature from *Borovsky et al.* [2013]) is defined as follows:

$$\mathrm{MC} \equiv \rho_M B_S / \rho_S B_M \tag{3}$$

The effect of the magnetospheric mass density on reconnection is diminished somewhat because the magnetospheric magnetic field magnitude is often larger than the magnetosheath magnetic field. Table 1 shows the MC and *R* values for the eight duskside magnetopause events, including the event in Figure 2.

The effect of enhanced magnetospheric convection on the mass density is evident in Table 1. Two events on 9 and 11 September 2015 with the highest *Kp* have the highest magnetospheric mass densities (although the second event on 19 September 2015 shows that the *Kp* and magnetospheric mass density are not necessarily correlated all the time). For the two magnetopause crossings on 9 and 11 September, the mass correction factors (MCs) are 10% and 29%, respectively. There were two very short periods in the magnetosphere where the extreme MCs were 15% (for the 9 September event) and 47% (for the 11 September event). These are the highest mass correction factors observed in the eight events, and they occur for only one 10 s ion spectrum each. The magnetospheric mass density was never greater than the magnetosheath mass density.

The two columns in Table 1 labeled "*R* avg" and "*R* extreme" quantify the reduction in the reconnection rate (equation (2)) for the average and extreme magnetospheric ion populations, respectively. The 11 September 2015 had an average and extreme reduction of 12% and 18% respectively. For all other events, the average reduction was <5%, and the extreme reduction was <7%.

## 5. Conclusions

Using eight duskside magnetopause crossings by the MMS spacecraft (Table 1), the effect of magnetospheric ions on magnetic reconnection was determined. All eight crossings occurred near high-shear reconnection X lines, so the magnetospheric plasma observed near the magnetopause probably represented the plasma that interacted with the reconnection diffusion region. For seven of eight events, total number densities of the ring current and warm plasma cloak populations were determined, and they were compared to number densities determined independently from plasma wave measurements from the MMS fields experiment. The consistency between the independent number density measurements indicates that there was little evidence of plasmaspheric plumes in seven of the eight events. It is likely that these plumes extend to the magnetopause in a region closer to the noon meridian, as illustrated in Figure 1 [*Walsh et al.*, 2013].

For most events, the ring current and warm plasma cloak magnetospheric ion populations had little effect on reconnection. *Wang et al.* [2015] reached a similar conclusion using only $O^+$ and $H^+$ observations from Cluster. From equation (2), there was a 5–7%

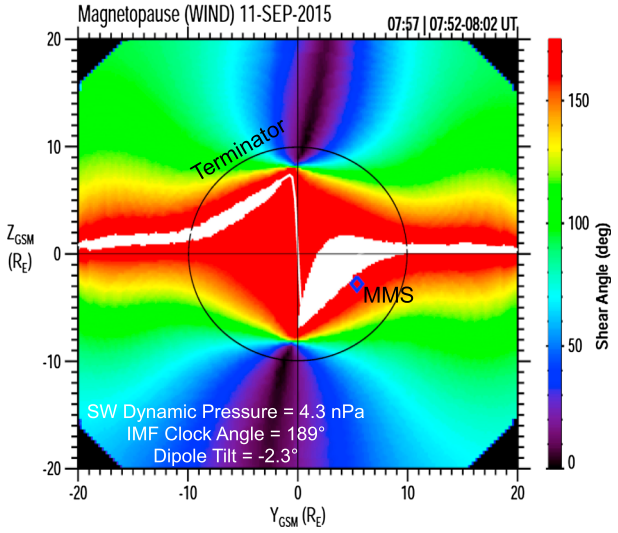


**Figure 3.** Modeled shear angles between the magnetosheath and magnetospheric fields for the magnetopause crossings in Figure 2. MMS crossed near a broad region where the shear angle was ~180°, indicating that the spacecraft were close to an antiparallel reconnection X line.

predicted reduction in the reconnection rate for seven of eight events. The 11 September 2015 event, shown in Figure 2, had the highest magnetospheric mass density of the eight events. For this event, the predicted average and extreme reductions in the reconnection rate were 12% and 18%, respectively. One cannot draw statistical conclusions from the limited number of events here, but these observations, combined with those from *Wang et al.* [2015], strongly suggest that moderate- and high-energy magnetospheric ions typically have little effect on reconnection. It remains to be seen if the plasmaspheric plume significantly affects reconnection near local noon. Also, it remains to be seen if there are higher warm plasma cloak densities on the dawnside magnetopause. Higher occurrence frequencies [*Chappell et al.*, 2008] and higher densities would make magnetospheric ions more important at the dawnside magnetopause.

**Acknowledgments**
The MMS mission required years of effort from a large number of women and men. Collectively, they share in the scientific successes of the mission. Solar wind data from the Wind spacecraft are from the CDAWeb. All data from the first 6 months of the mission will be available to the general public through the MMS website in March 2016.

## References

Birn, J., J. E. Borovsky, and M. Hesse (2008), Properties of asymmetric magnetic reconnection, *Phys. Plasmas*, *15*, 032101, doi:10.1063/1.2888491.

Borovsky, J. E., and M. H. Denton (2006), Effect of plasmaspheric drainage plumes on solar wind/magnetosphere coupling, *Geophys. Res. Lett.*, *33*, L20101, doi:10.1029/2006GL026519.

Borovsky, J. E., M. H. Denton, R. E. Denton, V. K. Jordanova, and J. Krall (2013), Estimating the effects of ionospheric plasma on solar wind/magnetosphere coupling via mass loading of dayside reconnection: Ion-plasma-sheet oxygen, plasmaspheric drainage plumes, and the plasma cloak, *J. Geophys. Res. Space Physics*, *118*, 5695–5719, doi:10.1002/jgra.50527.

Burch, J. B., T. E. Moore, R. B. Torbert, and B. L. Giles (2015), Magnetospheric multiscale overview and science objectives, *Space Sci. Rev.*, doi:10.1007/s11214-015-0164-9.

Cassak, P., and S. A. Fuselier (2015), Reconnection at Earth's dayside magnetopause, in *Magnetic Reconnection*, *Astrophys. Space Sci. Library*, vol. 427, edited by W. Gonzalez and E. Parker, Springer, Heidelberg, Germany.

Cassak, P. A., and M. A. Shay (2007), Scaling of asymmetric magnetic reconnection: General theory and collisional simulations, *Phys. Plasmas*, *14*, 102114, doi:10.1063/1.2795630.

Chappell, C. R., M. M. Huddleston, T. E. Moore, B. L. Giles, and D. C. Delcourt (2008), Observations of the warm plasma cloak and an explanation of its formation in the magnetosphere, *J. Geophys. Res.*, *113*, A09206, doi:10.1029/2007JA012945.

Collin, H. L., W. K. Peterson, J. F. Drake, and A. W. Yau (1988), The helium components of energetic terrestrial ion upflows: Their occurrence, morphology, and intensity, *J. Geophys. Res.*, *93*, 7558–7564, doi:10.1029/JA093iA07p07558.

Fuselier, S. A. (1995), Kinetic aspects of reconnection at the magnetopause, in *Physics of the Magnetopause*, *Geophys Monogr. Ser.*, vol. 90, edited by P. Song, B. Sonnerup, and M. Thomsen, pp. 181–187, AGU, Washington, D. C.

Fuselier, S. A., and W. Lewis (2011), Properties of near-Earth magnetic reconnection from in-situ observations, *Space Sci. Rev.*, *160*, 95–121, doi:10.1007/s11214-011-9820-x.

Fuselier, S. A., D. M. Klumpar, and E. G. Shelley (1991), Ion reflection and transmission during reconnection at the Earth's subsolar magnetopause, *Geophys. Res. Lett.*, *18*, 139–142, doi:10.1029/90GL02676.

Fuselier, S. A., E. G. Shelley, and D. M. Klumpar (1993), Mass density and pressure changes across the dayside magnetopause, *J. Geophys. Res.*, *98*, 3935–3942, doi:10.1029/92JA02236.

Fuselier, S. A., W. S. Lewis, C. Schiff, R. Ergun, J. L. Burch, S. M. Petrinec, and K. J. Trattner (2014), Magnetospheric multiscale science mission profile and operations, *Space Sci. Rev.*, doi:10.1007/s11214-014-0087-x.

Gosling, J. T., M. F. Thomsen, S. J. Bame, R. C. Elphic, and C. T. Russell (1990), Cold ion beams in the low latitude boundary layer during accelerated flow events, *Geophys. Res. Lett.*, *17*, 2245–2248, doi:10.1029/GL017i012p02245.

Labelle, J., R. A. Treumann, W. Baumjohann, G. Haerendel, N. Sckopke, G. Paschmann, and H. Lühr (1988), The duskside plasmapause/ring current interface—Convection and plasma wave observations, *J. Geophys. Res.*, *93*, 2573–2590, doi:10.1029/JA093iA04p02573.

McFadden, J. P., C. W. Carlson, D. Larson, J. Bonnell, F. S. Mozer, V. Angelopoulos, K.-H. Glassmeier, and U. Auster (2008), Structure of plasmaspheric plumes and their participation in magnetopause reconnection, First results from THEMIS, *Geophys. Res. Lett.*, *35*, L17S10, doi:10.1029/2008GL033677.

Olsen, R. C., S. D. Shawhan, D. L. Gallagher, J. L. Green, C. R. Chappell, and R. R. Anderson (1987), Plasma observations at the Earth's magnetic equator, *J. Geophys. Res.*, *92*, 2385–2407, doi:10.1029/JA092iA03p02385.

Sonnerrup, B. U. Ö., G. Paschmann, I. Papamastorakis, N. Sckopke, G. Haerendel, S. J. Bame, J. R. Asbridge, J. T. Gosling, and C. T. Russell (1981), Evidence for magnetic field reconnection at the Earth's magnetopause, *J. Geophys. Res.*, *86*, 10,049–10,067, doi:10.1029/JA086iA12p10049.

Su, Y.-J., J. E. Borovsky, M. F. Thomsen, R. C. Elphic, and D. J. McComas (2000), Plasmaspheric material at the reconnecting magnetopause, *J. Geophys. Res.*, *105*, 7591–7600, doi:10.1029/1999JA000266.

Torbert, R., et al. (2014), The FIELDS instrument suite on MMS: Scientific objectives, measurements, and data products, *Space Sci. Rev.*, *160*, 95–121, doi:10.1007/s11214-014-0109-8.

Torkar, K., R. Nakamura, M. Tajmar, C. Scharlemann, H. Jeszenszky, G. Laky, G. Fremuth, C. P. Escoubet, and K. Svenes (2014), Active spacecraft potential control investigation, *Space Sci. Rev.*, doi:10.1007/s11214-014-0049-3.

Trattner, K. J., J. S. Mulcock, S. M. Petrinec, and S. A. Fuselier (2007), Location of the reconnection line at the magnetopause during southward IMF conditions, *Geophys. Res. Lett.*, *34*, L03108, doi:10.1029/2006GL028397.

Walsh, B. M., D. G. Sibeck, Y. Nishimura, and V. Angelopoulos (2013), Statistical analysis of the plasmaspheric plume at the magnetopause, *J. Geophys. Res. Space Physics*, *118*, 4844–4851, doi:10.1002/jgra.50458.

Walsh, B. M., T. D. Phan, D. G. Sibeck, and V. M. Souza (2014a), The plasmaspheric plume and magnetopause reconnection, *Geophys. Res. Lett.*, *41*, 223–228, doi:10.1002/2013GL058802.

Walsh, B. M., J. C. Foster, P. J. Erickson, and D. G. Sibeck (2014b), Simulataneous ground- and space-based observations of the plasmaspheric plume and reconnection, *Science*, *343*, 1122–1125.

Wang, S., L. M. Kistler, C. G. Mouikis, and S. M. Petrinec (2015), Dependence of the dayside magnetopause reconnection rate on local conditions, *J. Geophys. Res. Space Physics*, *120*, 6376–6408.

Yau, A. W., B. A. Whalen, W. K. Peterson, and E. G. Shelley (1984), Distribution of upflowing ionospheric ions in the high-altitude polar cap and auroral ionosphere, *J. Geophys. Res.*, *89*, 5507–5522, doi:10.1029/JA089iA07p05507.

Young, D. T., et al. (2014), Hot plasma composition analyzer for the magnetospheric multiscale mission, *Space Sci. Rev.*, doi:10.1007/s11214-014-0049-6.